Chapter 5

Fabrication of NIR Sensitive-Low Operating Voltage Phototransistor with Unidirectional Organic Polymer

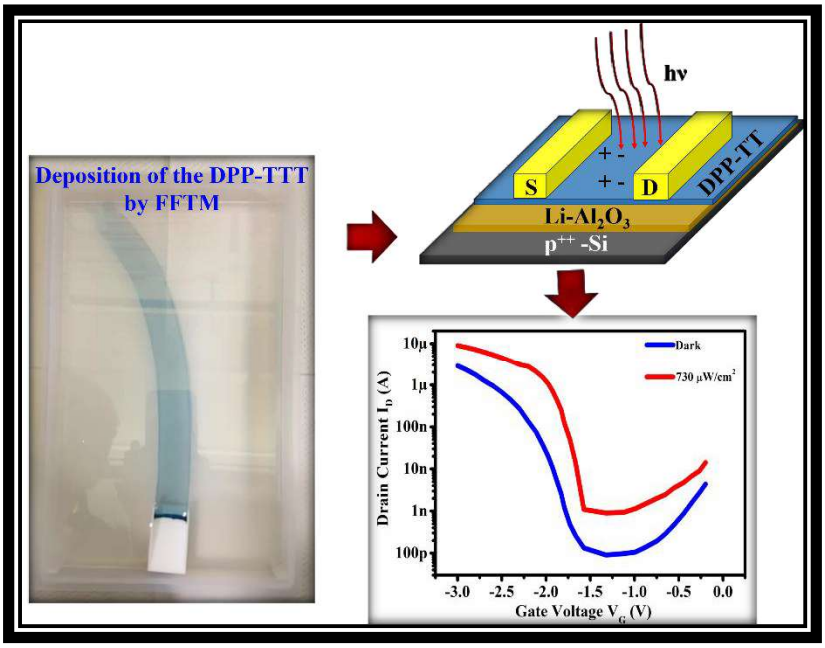

This chapter discusses the fabrication of a highly sensitive, low-voltage OPT utilizing a Li-Al_2O_3 ion-conducting dielectric. The use of this dielectric provides a high areal capacitance, enabling efficient low-voltage operation. The thin film of the organic semiconductor, DPP-TTT, was fabricated using the UFTM. The resulting OPTs exhibit excellent performance, particularly in terms of responsivity, detectivity, and sensitivity.

5.1. Introduction:

The demand for phototransistors has grown significantly due to several factors. One key driver is the increasing adoption of optical sensing and detection technologies in various industries such as telecommunications, automotive, medical, and consumer electronics [136]. Phototransistors play a crucial role in these applications by converting light signals into electrical signals, enabling the detection and analysis of light in a wide range of conditions. The increasing focus on energy efficiency and the utilization of renewable energy sources has prompted the development of photovoltaic systems and solar energy harvesting [137], where phototransistors may play a crucial role due to their capability to convert light into electrical energy [138]. Moreover, the advancements in communication systems and imaging technologies have created a growing demand for high-performance NIR-sensitive phototransistors [139] where devices need to be highly sensitive with a high signal-to-noise ratio. Despite a wide range of applications NIR-organic photodetectors (NIR-OPTs) have received less attention in research [28] due to the limited availability of stable photoactive organic materials that exhibit both high NIR absorption with high carrier mobility. Therefore, the performance of NIR-OPTs has remained unsatisfactory up to this point. Currently, a number of groups are using inorganic or inorganic/organic hybrid as active layers for the NIR photodetector device fabrication [106, 140-142]. However, OPTs offer several advantages over inorganic or silicon-based transistors due to its solution processability as well as low cost fabrication[143, 144]. This makes OPTs fabrication more economical compared to complex and expensive fabrication processes involved in inorganic or silicon-based transistors and OPTs can be fabricated over large areas, enabling the development of large-area and high-resolution photodetection arrays[145]. OPT can be fabricated using solution-based processes, such as coating techniques, which are low cost and scalable. Despite the lower costs associated with the processing, and fabrication

of organic semiconductors, the synthesis of these organic semiconductors or molecules remains expensive, moreover, the stability of organic semiconductors is a critical concern [146, 147]. Consequently, it is crucial to minimize wastage of material during the device fabrication process. Conventional methods such as dip coating, blade coating, spray coating, and spin coating result in significant polymer solution waste, contributing to higher overall costs [48]. To address this issue, some cost-effective mehods such as Floating Film Transfer Method (FTM) and Unidirectional Folating Film Transfer Method (UFTM), have been used to reduce polymer solution wastage during processing, ultimately lowering the fabrication costs [47] and achieve more efficient use of materials, thereby making the fabrication of organic semiconductor devices more economically viable. [148, 149].

Till now the groups who are working OPTs are using SiO_2 as a dielectric material that requires high operating voltage (>30 V) [134, 150, 151]. However, for portable optoelectronics devices, it's really urgent to develop low operating voltage OPTs that has lower energy consumption as well and improves the safety of electronic devices [152]. Therefore, a suitable high dielectric constant (high-κ) material is required to reduce the operating voltage of the OPTs. Therefore, a number of high-k dielectric such as ZrO_2[153], Li_2ZnO_2[154], MgZnO[155], and LaZrOx[156], are reported for various organic transistor device fabrication. Among various types of organic semiconductors, DPP-TTT is an emerging NIR absorbing material to use the photosensitive channel of an OPT. A few numbers of phototransistor devices have been also reported using the DPP-TTT molecule. However, those OPTs require high operating voltage and show low responsivity [28, 157]. Hence, fabricating OPTs with low operating voltage and high NIR sensitivity is essential for commercial application. In this work, low voltage (OPT) has been fabricated with a sol-gel derived Li-Al_2O_3 ion-conducting gate dielectric where DPP-TTT has been used as a photoactive channel layer, fabricated via UFTM which forms a unidirectional organic film

at the air-liquid interface, as shown in the schematic diagram of ***Figure 3.1***. The device fabricated by UFTM enhances the film's crystallinity and grain orientation, enhancing charge carrier transportation and sensing performance of the phototransistor [47]. This organic film was transferred on Li-Al_2O_3 gate dielectric coated p^+-Si substrate [158], which enabled us to deposit large-area oriented organic thin film with good uniformity. Which is desirable for practical applications. The operating voltage of this OPT is favorable to 2 V by maintaining its high NIR sensitivity and responsivity.

5.2. Materials and Methods:

5.2.1. Materials:

Aluminium nitrate nonahydrate Al $(NO_3)_3.9H_2O$, Lithium acetate (CH_3COOLi), have been used as precursor materials for synthesis Li-Al_2O_3 gate dielectric whereas 2-methoxy ethanol (purchased from SDFCL) used as a solvent. The commercial polymer of DPP-TTT with a molecular weight of 83 KDa (Purchased from Ossilla) has been used for semiconducting channel material of OPT, and chloroform, glycerol, and ethylene glycol (purchased from Sigma Aldrich) used for film fabrication.

5.2.2. Dielectric Synthesis:

The Lithium Alumina (Li-Al_2O_3) dielectric solution was synthesized as given in the ***chapter 2 section (2.3.2.1)***

5.2.3. Device Fabrication:

OPTs were fabricated using 15×15 mm substrates of highly p-doped silicon (p^{++}-Si), as shown in ***Figure 5.1.*** Initially, these substrates were cleansed sequentially with deionized (DI) water, Acetone, and Isopropanol, each in an ultrasonic bath for a duration of 15 minutes. After this cleansing step, they were dried in an atmosphere of nitrogen before being transferred to a chamber for oxygen plasma treatment. In this chamber, the substrates

were subjected to oxygen plasma for a period of 10 minutes to eliminate any remaining hydrocarbons and to increase the surface's hydrophilicity. Following the preparation phase, the substrates were coated with a Li-Al_2O_3 precursor solution through spin-coating. This solution was filtered beforehand using a 0.45 µm PVDF syringe filter to eliminate any sizable particles. This coating was applied at a speed of 5000 rpm for 50 seconds and subsequently heated on a hot plate set to 90 ºC, as outlined in the methodology of reference*[159]*. Following spin-coating, the substrates were annealed at 350 ºC for 30 minutes, a procedure that was repeated two times. A final annealing stage at 500 ºC for one hour was conducted to obtain the requisite thickness of the Li-Al_2O_3 dielectric thin film. To finalize the process, the substrates were conditioned with HMDS within a closed petri dish containing a single drop of HMDS, ensuring the substrates attained hydrophobic properties, to make the good adhesion between Li-Al_2O_3 layer and organic DPP-TTT film. The thin film of the DPP-TTT was fabricated by using cost-effective method, *UFTM*. This method comprises steps of preparation of a warm (40 °C) hydrophilic liquid mixture of ethylene glycol and glycerol (1:1 in V/V); spreading around 10-15 µl of the hydrophobic DPP-TTT nanohybrid solution, 'CP ink', onto the surface of the liquid substrate; lifting the developed thin solid film floating over the air-liquid interface over substrates of choice; thorough washing of the films with methanol and (IPA) to remove any liquid residue and then annealing at 110 °C under N_2 atmosphere to fabricate the final thin film [125]. In this method, the spontaneous spreading of the polymeric solution was governed by the Marangoni effect, and to guide the spreading in one direction, a Teflon slider was used, as illustrated in ***Figure 2.5.*** During the spreading of the solution, chloroform evaporated rapidly, and a dried, thin solid film was found floating like a semi-transparent ribbon Figure. Notably, UFTM films of conducting polymers (CPs) that contain hydrophobic alkyl side chains, exhibits a preference for adopting an edge-on type molecular packing.

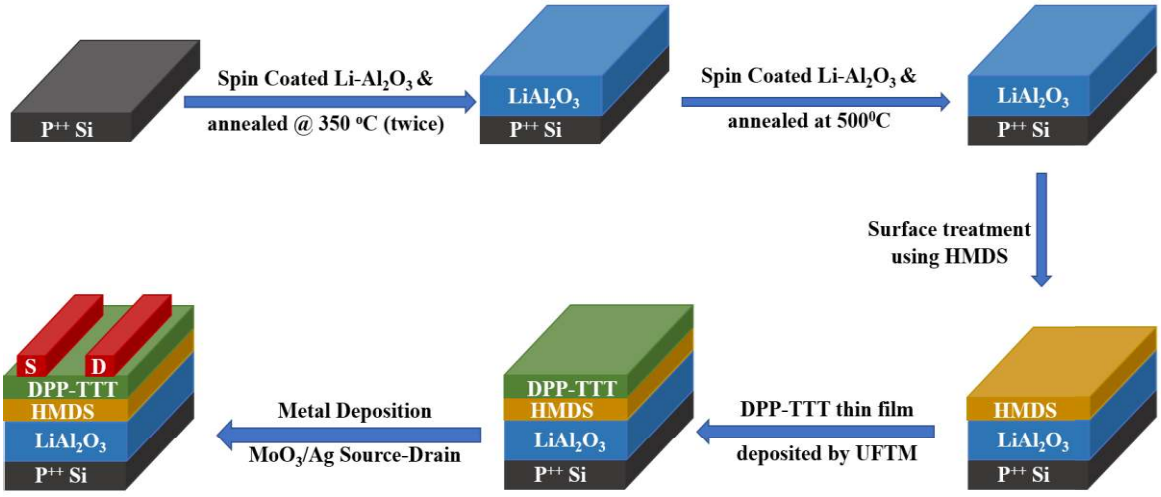

Figure 5. 1 *Schematic diagram of Li-Al_2O_3/DPP-TTT OFET fabrication.*

5.3. Results and Discussion:

5.3.1. Dielectric Characterizations:

5.3.1.1. XRD Analysis:

To determine the structural properties of the Li-Al_2O_3 dielectric the thin samples were prepared using spin coating and annealing at silicon substrate for GIXRD measurement. No major peak has been observed in the GIXRD pattern of the Li-Al_2O_3 thin film as shown in ***Figure 5.2(a),*** reveals the amorphous nature of the Li-Al_2O_3 dielectric thin film [159, 160].

5.3.1.2. Optical Analysis:

The optical transmittance spectra of the Li-Al_2O_3 dielectric thin film were measured using UV-Visible spectroscopy. The thin film was deposited on a quartz substrate under the same conditions used for the fabrication of OPT and MIM devices. As shown in the ***Figure 5.2(b)***, the film exhibits over 85% transparency across the visible range (200-800 nm) of the electromagnetic spectrum, making it suitable for wide band gap materials. This high level of transparency suggests minimal scattering within the film, particularly in the visible

to NIR region. Scattering in thin films can arise due to imperfections such as defects, voids, impurities, or surface roughness. As such, the data suggest that the film has a minimal presence of these imperfections, which contributes to a reduced leakage current. This is a crucial factor for achieving high-performance gate dielectrics in thin-film transistors (TFTs).

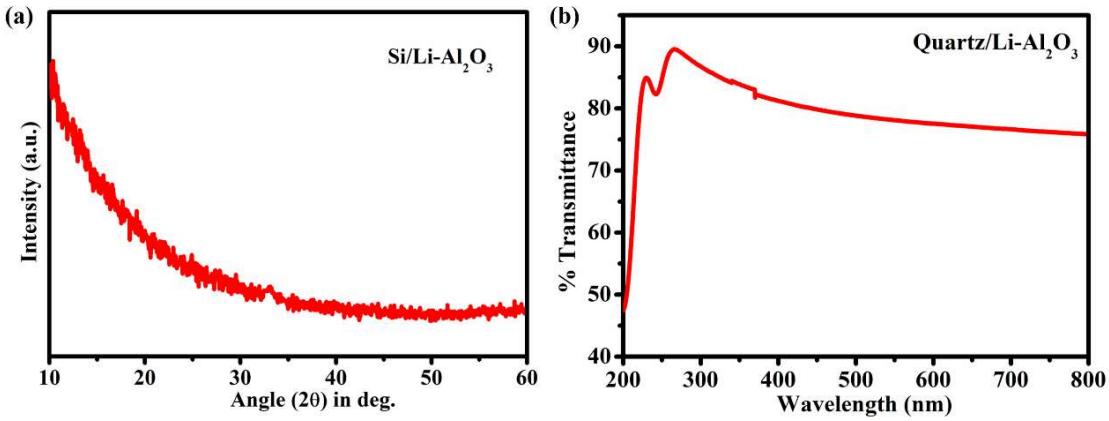

Figure 5. 2 (a) *GIXRD pattern of the Li-Al_2O_3 thin film* ***(b)*** *UV-spectrum of the dielectric thin film.*

5.3.1.3. Surface Characterization:

AFM measurements were done to confirm the surface roughness of the dielectric film. 2 D and 3 D AFM images of Li-Al_2O_3 thin film have been depicted in ***Figure 5.3 (a) & (b),*** respectively. The extracted RMS roughness of the dielectric film is 0.23 nm. This study suggests that the dielectric surface exhibits remarkably low roughness, attributed to the amorphous quality of dielectric thin films. The characteristics could prove highly advantageous in producing high performance TFTs [161, 162].

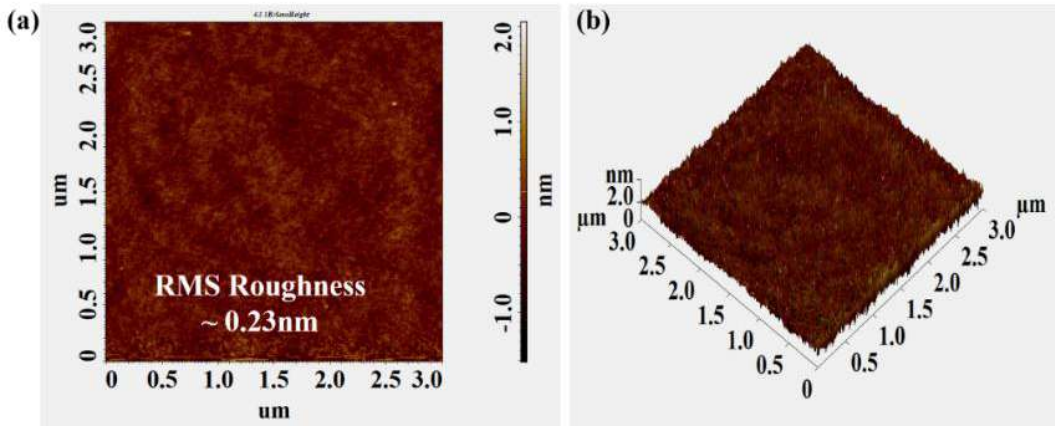

Figure 5. 3 (a) *2D AFM image* ***(b)*** *3D image of the Li-Al2O3 dielectric thin film.*

5.3.1.4. Leakage Current and Areal Capacitance Measurement:

To determine the electrical properties of the solution processed Li-Al_2O_3 ion conducting dielectric we fabricate device with MIM structure as shown in the inset of ***Figure 5.4 (a).*** It shows the leakage current density 1.2×10^{-7} upto 30 V which indicates very low leakage current. Which shows the good insulating behaviour of the Li-Al_2O_3 dielectric. Additionally, the capacitance vs. frequency (C-f) measurement of Li-Al_2O_3 dielectric has been performed in Metal-insulator-metal (MIM) as shown in ***Figure 5.4 (b).***

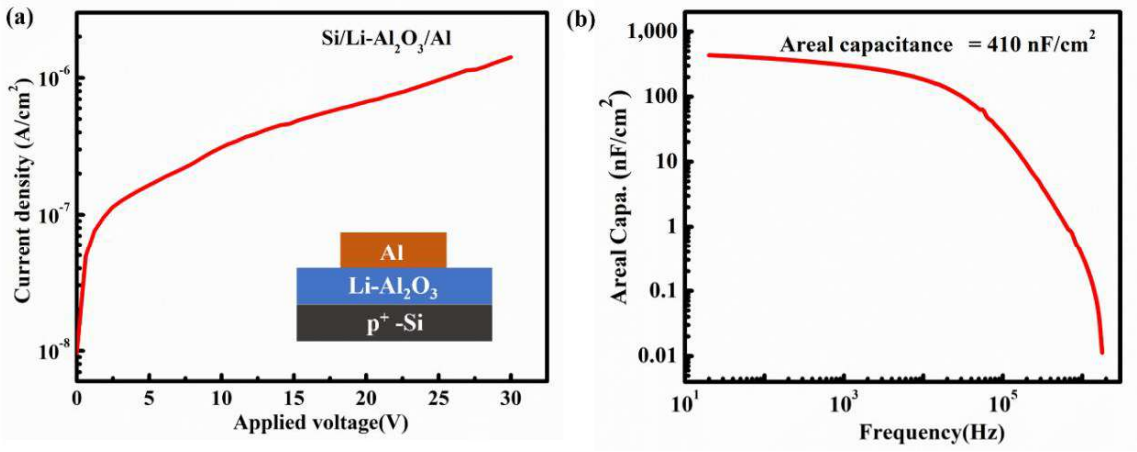

Figure 5. 4 (a) *Leakage current versus applied voltage Li-Al_2O_3 dielectric thin film,* ***(b)*** *capacitance vs. frequency plot of Li-Al_2O_3 dielectric thin film in Metal-Insulator-Metal (MIM) geometry*

The areal capacitance of the Li-Al_2O_3 thin film is 410 nF/cm^2 at 50 Hz operating frequency. This high value of the areal capacitance is due to mobile Li^+-ion in the Li-Al_2O_3 thin film in low-frequency region [163, 164]. The areal capacitance experiences a gradual decrease up to 10^4 Hz, followed by a sharp decline thereafter. This phenomenon occurs because the mobile Li^+-ions cease to contribute to ionic Polarization.

5.3.2. DPP-TTT Thin Film Characterizations:

5.3.2.1. XRD Analysis:

Grazing Incidence X-ray diffraction (GIXRD) analysis was conducted to verify the orientation of the polymer backbone chains using in plane as well as out of plane as illustrated in ***Figure 5.5(a) and Figure 5.5(b),*** respectively. The study focused on UFTM-casted films on quartz substrates, revealing distinct peaks at 4.4°, 8.6°, and 17.6°, which correlate to the (100), (200), and (300) planes, respectively. The presence of (h00) peaks upto 3rd order confirms the edge-on orientation and molecular ordering of the DPP-TTT polymer semiconductor, indicative of the beneficial alignment for charge carrier transport in high mobility OPTs devices.

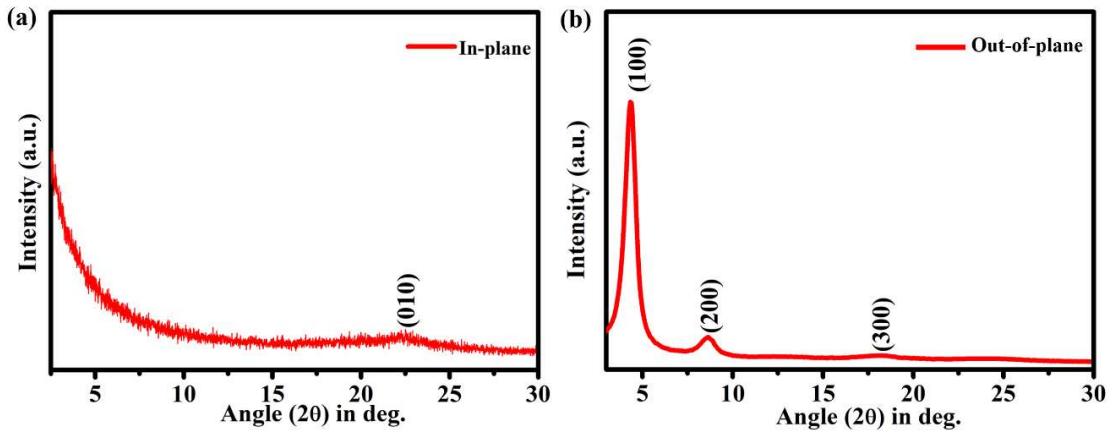

Figure 5. 5 *GIXRD pattern of* ***(a)*** *in plane, and* ***(b)*** *out of plane DPP-TTT thin film.*

5.3.2.2. Optical Analysis:

For the optical characterization of the DPP-TTT semiconducting layer, polarized UV-Visible spectroscopy was utilized on samples deposited on quartz glass via UFTM as shown in inset of ***Figure 5.6 (a)***. The DPP-TTT film exhibited two significant absorption peaks at 814 nm (attributed to the π-π* transition) and a vibronic shoulder at 748 nm as shown in ***Figure 5.6(b).*** The molecular orientation was assessed by orienting the film parallel and perpendicular to the polarizer, and determining the dichroic ratio (DR) as DR = $(A_{\parallel})/(A_{\perp})$, where $(A_{\parallel})$ and $(A_{\perp})$ represent the absorption intensities with the polarizer aligned parallel and perpendicular to the polymer chain orientation, respectively. The observed DR Values of 1.61 at 214nm and 1.76 at the shoulder peak confirmed the molecular orientation within the films as shown in ***Figure 5.6 (b).***

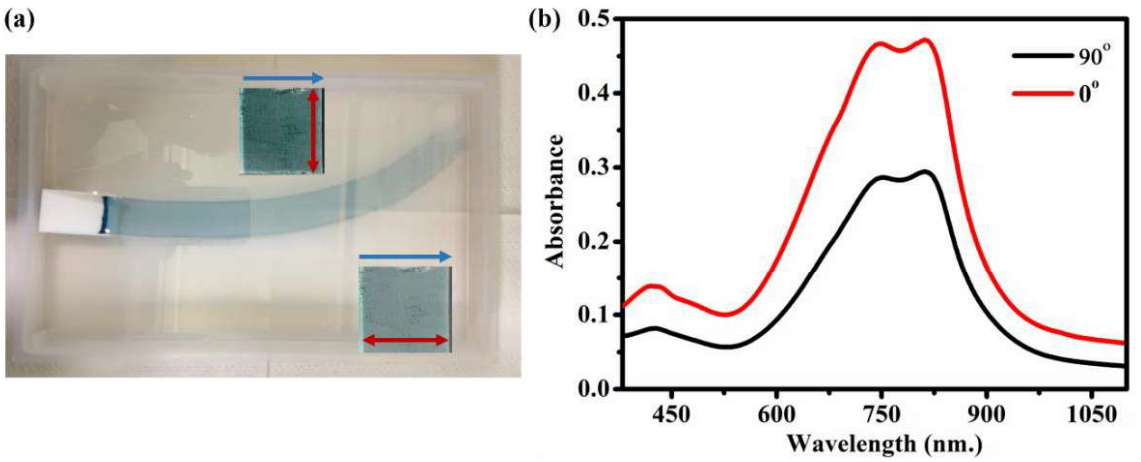

Figure 5. 6 (a) *UFTM thin film image and in inset thin film transferred on quartz substrate in which blue arrow shows the direction of flow and double-sided red arrow shows the polarizer direction* ***(b)*** *polarized visible/NIR absorption spectra of DPP-TTT thin film.*

5.3.2.3. Surface Characterization:

Additionally, Atomic Force Microscopy (AFM) provided insights into the surface morphology and chain orientation of the polymer film, further deposited on a highly doped silicon substrate for this purpose. This study clearly shows the molecules of the film are

stacked in a unique direction of the film which is indicated by the arrow mark, as shown in ***Figure 5.7(a)*** also providing the evidence of unidirectional growth of the film by this deposition method. The thickness of the film was also identified by this AFM study which is around 30±0.0253 nm and roughness profile is shown in ***Figure 5.7(b),*** and the average roughness is around 3±0.015 nm.

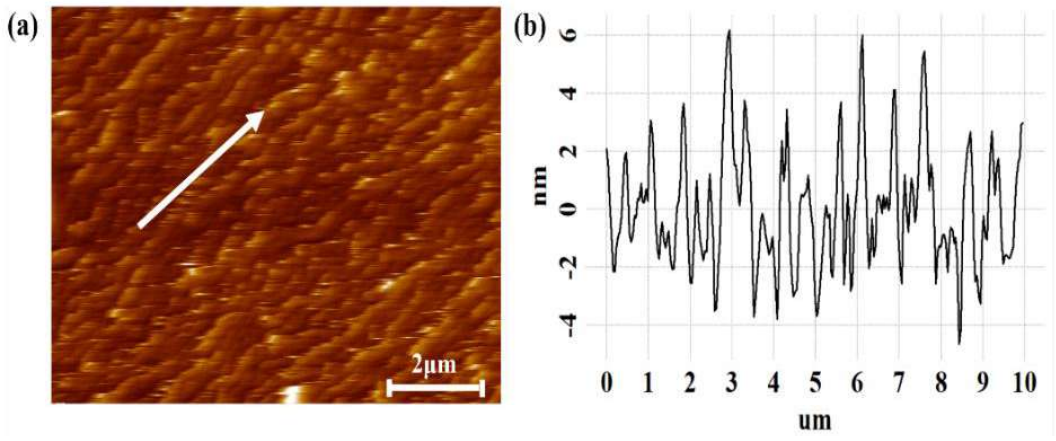

Figure 5. 7 (a) *AFM image of DPP-TTT thin film* ***(b)*** *Roughness profile of the DPP-TTT thin films.*

5.3.3. Electrical Characterizations:

The fabrication of the OPTs utilized a bottom-gate top-contact structure, with a width-to-length (W/L) ratio of 33.3, with dimensions of W=1 mm and L=30 µm. These devices were tested under normal room conditions, maintaining a relative humidity around 50%. Device output and transfer characteristics were measured for both samples when the orientation was parallel, and perpendicular to the channel as shown in ***Figure 5.8 (a).*** The observed output characteristics in ***Figure 5.8 (b) 5.8 (c)*** and transfer characteristics, in ***Figure 5.8 (d),*** confirm the p-channel behavior of the devices, capable of operating up to a ~2-3 V external bias. Notably, the output characteristics in ***Figure 5.8 (b)*** reveals that drain current (I_{DS}) reaches saturation around -1 V drain voltage (V_D). The saturation mobility and threshold voltage were derived from linear fit of the square root of I_{DS} versus gate voltage

V_G, as illustrated in ***Figure 5.8 (d)*** using ***equation 5.1*** for calculating mobility.

$$I_{DS} = \frac{W\mu_{sat}C_{ox}}{2L}(V_{GS} - V_{TH})^2 \quad \text{..... (5.1)}$$

In this equation $I_{DS,}$ is the notation for the saturation drain current. threshold at which significant conduction starts within the device. Additionally, the terms L and W are the length and width of the channel, respectively, while μ_{sat} is used to denote the field-effect mobility. The abbreviations V_D and V_G refer to the drain voltage and source voltage, respectively. Analysis of the device's performance indicated a threshold voltage near -1.8 V and a hole mobility of approximately 0.21 cm²/V·s for parallel aligned and for perpendicular aligned is 0.015 cm²/V·s, marking impressive functionality for a low-voltage transistor based on organic polymers.

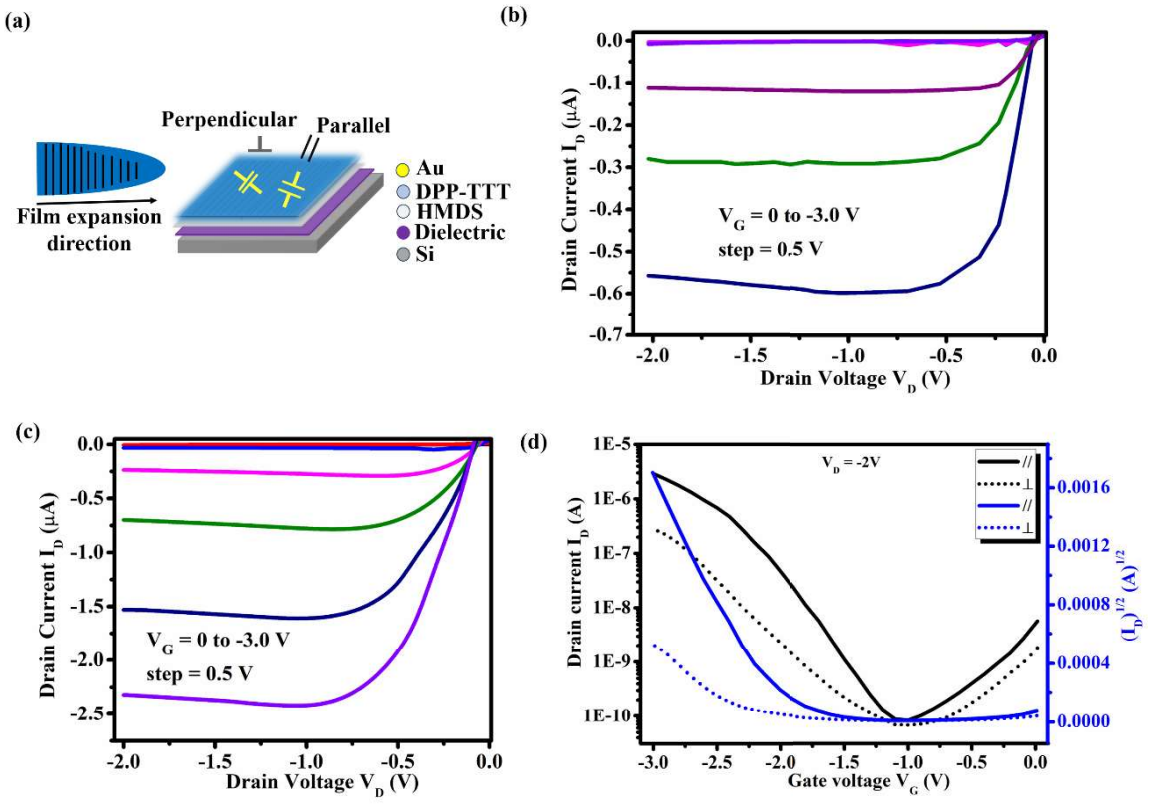

Figure 5. 8 (a) *Schematic for the channel orientation,* ***(b)*** *Output characteristics of Perpendicular* ***(c)*** *output characteristics of Parallel,* ***(d)*** *Transfer characteristics of OFETs with* $(I_D)^{1/2}$ *Vs.* V_G.

5.3.3.1. Optical Sensing of OPTs:

Furthermore, OPTs were investigated under different wavelengths and light was exposed to the active channel as shown in ***Figure 5.9 (a).*** The sensor responds very poorly to other wavelengths also plotted over different wavelengths from 440 -750 nm in the visible range, as shown in ***Figure 5.9 (b),*** indicating this device can work as a NIR selective photodetector, which is also supported by the UV-visible spectrum of the DPP-TTT as *shown in* ***Figure 5.6 (b).*** So, we continued all the optical sensing at 830nm wavelength. The photosensitivity of these OPTs has been investigated under dark and near-infrared (NIR) light irradiation of a specific wavelength of 830 nm, with an intensity ranging from 120 to 730 $\mu W/cm^2$.

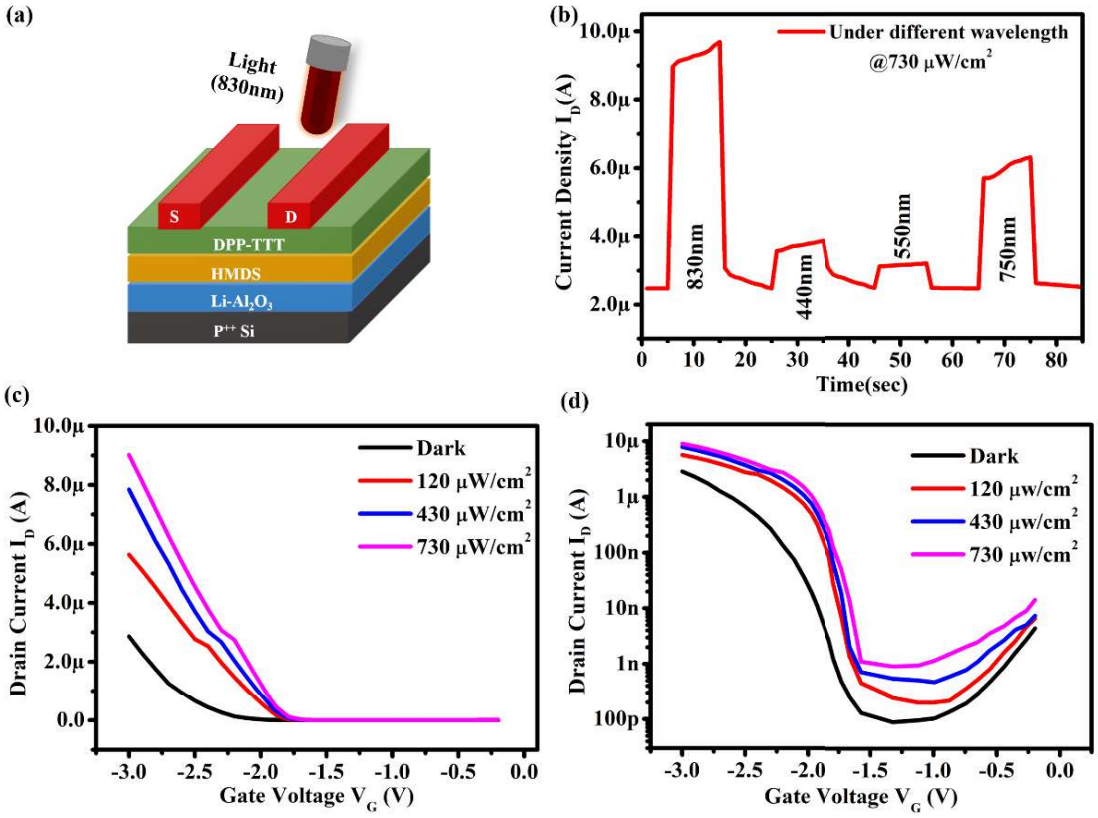

Figure 5. 9 ***(a)*** *represents the device schematic under light exposure* ***(b)*** *Photocurrent versus time of OFET under Different wavelengths of light.* ***(c)*** *Transfer characteristics of OFET under different power Intensity of light,* ***(d)*** *plotted graph in log (10) plot of Transfer characteristics in Dark and Under light illumination of different power of light in ($\mu W/cm^2$).*

Transfer characteristics of OPT clearly indicate that current of the device increases with light intensities in both accumulation and depletion mode as shown in ***Figure 5.9 (c) and 5.9 (d)***. Moreover, the change of depletion mode current is significantly higher than the accumulation mode current. In addition, it has been observed that the threshold voltage (V_{th}) of the device shifted toward a positive direction with light intensity as shown in ***Figure 5.10 (a).*** Both the enhancement of I_D and shifting of V_{th} originated due to the photogenerated charge carriers (electron and hole) by the incident light, which is clearly observed even under low light intensity like 120 $\mu W/cm^2$, indicating high NIR sensitivity of this OPT. After absorbing NIR light by the channel semiconductor of OPT, photo-generated excitons separate into free charge carriers, namely holes and electrons. These photogenerated holes added the carrier concentration of the channel that enhanced the accumulation mode drain current (I_D), whereas photogenerated electrons are more static under such operation and shifted V_{th} of the device in a positive direction. When devices move towards depletion mode, these photogenerated electrons become conducting, which essentially decreases the sheet resistance of the organic semiconductor channel, resulting in an enhancement of the 'off current'[165].

Further responsivity (R),photosensitivity (S) , and specific detectivity (D) of this OPT have been calculated by the following equation (***Eq-1.11, 1.12 and 1.13***)[166, 167].

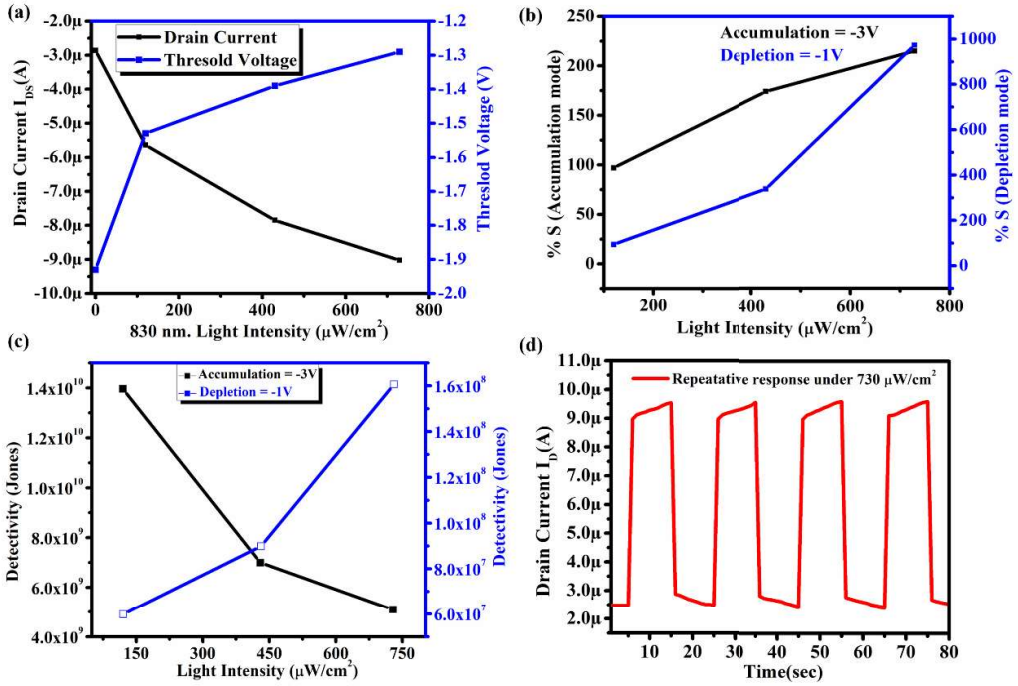

Figure 5. 10 (a) *Threshold voltage and Darin current under different illumination power. (b, & c) sensitivity, and detectivity v/s light intensity in accumulation and depletion mode respectively, (d)) Transient response of the device under 830nm at 730μW/cm².*

Table 5.1: Summary of the OFET Parameters

Light intensity (μW/cm²)	Drain Current (I_D) (μA)	Photosensitivity (Accumulation at -3V) (S) (%)	Photosensitivity (Depletion at -1V) (S) (%)	Responsivity (R) (A/W)	Specific Detectivity (D^*) (Jones)
Dark	-2.86	-	-	-	-
120	-5.64	97	95	76.94	1.4×10^{10}
430	-7.85	174	338	38.60	6.99×10^{9}
730	-9.02	215	973	28.16	5.09×10^{9}

The photosensitivity in accumulation and in depletion mode of the device have been plotted in ***Figure 5.10 (b)***, which shows that, in depletion mode sensitivity of the device is more efficient than accumulation mode operation, particularly at higher intensity. The sensitivity

under the lower intensity of (120 μW/cm^2) by NIR illumination is ~ 97 and 95% under accumulation and depletion mode of operation, whereas these sensitivities at a higher intensity (730 μW/cm^2) are 215 and 973%, respectively.

The observed change in current under light exposure is more pronounced in depletion mode than in accumulation mode, which can be elucidated through the interplay of photovoltaic and photoconductive effects within the semiconductor[168]. In depletion mode, the semiconductor channel is initially devoid of free carriers. Upon exposure to light, photons are absorbed, and electron-hole pairs are generated. The photogenerated holes are then able to contribute significantly to the conductivity, as they provide a substantial increase in the carrier population of the previously depleted channel. This influx of carriers leads to a marked increase in current due to the photovoltaic effect, where the semiconductor material itself acts like a photo-diode, generating a voltage and current upon light exposure. Concurrently, the photoconductive effect also plays a crucial role[169]. This effect describes an increase in the semiconductor's electrical conductivity attributable to the photon-induced generation of additional charge carriers. In depletion mode, this increase in conductivity is more noticeable because the baseline dark conductivity is very low; hence, any additional carriers have a significant impact. Conversely, in accumulation mode, the channel already possesses a high density of carriers. Therefore, the relative increase in conductivity and thus the change in current caused by additional photogenerated carriers is less dramatic. The detectivity of this device is ~ 1.4 ×10^{10} and 5.9 x 10^7 Jones at lower intensity (120 μW/cm^2) in accumulation and depletion mode, respectively which is reasonably high as NIR detector ***Figure. 5.10 (c)***. However, the detectivity of this OPT has been reduced to ~ 5.09 ×10^9 Jones at higher intensity (730 μW/cm^2). The photosensitivity, responsivity and specific detectivity of the device at different NIR intensities have been summarized in ***Table-5.1***. Overall performance of this OPT has been compared with other

reported OPT and has been summarized in ***Table-5.2***. This comparison clearly shows that the fabricated OPT has achieved a quite good performance by maintaining its low operating voltage which is mostly due to the unidirectional growth of the DPP-TTT organic semiconductor channel.

Table 5.2: Comparative study of current work with previously reported.

S.No.	Techniques	Operation Voltage	Mobility ($cm^2/V.s$)	Intensity	Responsivity (A/W)	Remark
1	Spin Coating	-5	0.08	0.91 mW/cm^2	11.59	Low mobility [170]
2.	PDMS	-60	$5*10^{-3}$	47.1 mW/cm^2	0.44	Low Responsivity [67]
3.	Spin coating	-100	$2.1*10^{-3}$	5 mW/cm^2	120	High voltage operated [134]
4.	Spin coating	-50	10^{-4}	180 mW/cm^2	-	Low mobility [133]
5.	**UFTM**	**-3**	**0.212**	**729 $\mu W/cm^2$**	**28.16**	**This Work**

The repetitive transient response of a phototransistor refers to its behavior during the transition from one light intensity level to another. It describes how the phototransistor reacts to changes in incident light and how quickly it settles into a new steady-state response [171]. The dynamic response of this OPT under NIR (830 nm) light illumination of intensity 730 $\mu W/cm^2$ has also been shown in ***Figure 5.10 (d)*** which indicates the rise time of this device is ~ 1 sec whereas the recovery time is ~1 sec.

5.4. Conclusion:

In this work a low operating voltage, NIR sensitive Organic phototransistor (OPT) has been fabricated by using a DPP-TTT organic polymer. The device fabrication has been done by

cost effective technique which include sol-gel derived Li-Al_2O_3 dielectric that shows a capacitance of 410 nf/cm^2 which is appropriate for low voltage operation (≤2.0 V). Besides, the unidirectional organic semiconducting layer has been fabricated by an 'unidirectional floating film transfer method'. Such a unique deposition technique is capable of growing an oriented growth of organic film with a significant Dichroic ratio of 1.76 of the polymer chain which helps to improve the charge transfer through the channel, resulting in a carrier mobility of 0.21 cm^2/V.s. The phototransistor shows good photosensitivity (97%) at low power of NIR 120 μW/cm^2 and good photoresponsivity of ~ 77 (A/W) as well as good specific detectivity of 1.4×10^{10} under accumulation mode. Overall, this work demonstrated a unique way to fabricate high-performance OPT by maintaining its operating voltage within 2.0 V